

# **Parametric Study on Reinforced Concrete Deep Beams Strengthened in Shear Using FRP**

**F.B.A. Beshara, T.S. Mostafa, A. S. Abd El-Maula, and M.G. Fathi**  
Civil Engineering Dept., Faculty of Engineering, Shoubra, Benha University

## **Abstract**

In this paper, finite element modeling and nonlinear analysis studies for reinforced concrete deep beams strengthened in shear using FRP sheets and strips, illustrated using the general-purpose ANSYS computer program. The parametric shear studies include the effect of FRP parameters (thickness of FRP sheets and strips, angle of FRP sheets and strips, length of FRP sheets, spacing between FRP strips and FRP material type) on the shear response of strengthened deep beams. It is predicted that the increase of thickness of FRP sheets or strips improves the deep beam shear capacity and the secant stiffness. Strengthening deep beam with CFRP upgrades the shear capacity more than strengthening with GFRP. An enhancement in the shear capacity and secant stiffness is noticed by strengthening with FRP, applied perpendicular to the predicted shear crack. The shear strengthening performance of FRP sheets or strips increases as the strengthening length increases.

**Keywords:** Reinforced concrete; Deep beams; Fiber reinforced polymers; Load-deflection curves; Load-steel strain curves; Finite element; ANSYS.

## **1. Introduction**

Deep beams are fairly commonly used as load distribution elements such as transfer girders, tank walls and foundation walls, often receiving many concentrated loads and transferring them to a small number of reaction points. Many experimental studies were made [1-6] on the structural response of reinforced concrete deep beams strengthened using CFRP, GFRP and other FRP composite materials. The main findings are that all strengthened deep beams give an enhancement in the ultimate load capacity with respect to reference models. The FRP laminates aligned at an angle of 45 degrees to the longitudinal axis of the deep beam are more effective than the horizontal and vertical ones in enhancing the ultimate load capacity of the deep beam. Furthermore, the ultimate load capacity of strengthened deep beams increases as the FRP strengthening length increased. Finally, the U-wrapped FRP sheets are shown to be very effective more than FRP side bonding in enhancing ultimate load capacity, ductility and initial stiffness due to an anchorage effect.

The aim of this paper is to present the results of parametric shear studies on the performance of reinforced concrete deep beams strengthened by FRP composite materials using ANSYS computer program [7]. Numerical model was developed [8] and used successfully to predict the experimental results in the literature. The main parameters include the effect of FRP sheets parameters such as thickness of FRP sheets, angle of FRP fibers, length of FRP sheets and material type of FRP sheets, and the effect of FRP strips parameters such as thickness of FRP strips, angle of FRP strips, spacing between FRP strips and FRP strips material.

## **2. Modeling and Evaluation Criteria**

### **2.1 Finite Element Geometric and Material Idealization**

The finite element modeling and nonlinear analysis is performed using ANSYS software [7]. The structural element types used to discrete the different materials are given in Table 1. The formulation of the related elements is given in [7,8]. For concrete in compression, a multi-linear compressive uniaxial stress-strain curve is used [9]. For concrete in tension, a linear constitutive law with linear-tension softening curve is used [10]. Bilinear stress-strain curve is adopted for steel reinforcement in compression and tension [8]. Nonlinear incremental-iterative solution technique is used to follow material nonlinearities in compression and tension.

### **2.2 Evaluation Criteria of the Parametric Studies**

In order to study the effect of different parameters affecting the behavior of reinforced concrete deep beams strengthened with FRP, series of deep beams; labeled (P1, P2, P3, P4, ..... to P13), have been analyzed. From the predicted load-deflection curves and load-steel strain curves for deep beams, the effects of the analyzed parameters have been studied using the following measures:

- Loads at the cracking level ( $P_{cr}$ ) and at the ultimate level ( $P_u$ ).
- Deflection at the cracking level ( $\Delta_{cr}$ ) and at the ultimate level ( $\Delta_u$ ).
- Secant stiffness ( $K_u$ ) = the ultimate load per unit displacement ( $P_u / \Delta_u$ ).
- Strain ductility ( $\mu_s$ ) = ultimate steel strain ( $\epsilon_u$ ) / yield strain ( $\epsilon_y$ ).

The input data of the main parameters are illustrated in Tables (2) and (3).

## **3. Effect of FRP Sheets Parameters**

The effects of FRP sheets thickness, FRP fibers angle, FRP sheet length and FRP material are investigated. The input data for the sensitivity studies are given in Table 2. The basic specimens used in this section, are the deep beam (P1) that has no FRP sheets, and the deep beam (P2) which strengthened with CFRP sheets. The testing results for these beams are reported in [5]. Typical geometrical details and 3-D finite element models are shown in Figure (1) for deep beams (P1, P2, P3, P4, P5 and P7).

### 3.1 Thickness of FRP Sheets

Three deep beams strengthened with different fiber thickness of FRP sheets are analyzed. The deep beam P1 is the un-strengthened specimen. For deep beams P2 and P3, the sheet thickness is considered as 0.17mm and 0.34mm respectively. The numerical load-deflection curves and load-steel strain curves for the deep beams are plotted in Figure (2). The following points are obtained from the comparison of strengthened deep beams (P2 and P3) with respect to control reference deep beam P1:

1. The increase of FRP sheets thickness improves the shear capacity at all levels. An enhancement in the shear capacity by 79% and 138% has been observed for specimen P2 and P3 respectively when compared with P1 at the cracking level, and by 69% and 85% at the ultimate level.
2. The mid-span deflection at all levels is increased by increasing FRP sheets thickness. At the cracking level, the deflection ( $\Delta_{cr}$ ) is increased for specimens P2 and P3 by 39% and 61% respectively. Also, the mid-span deflection at the ultimate level ( $\Delta_u$ ) is improved for P2 and P3 by 40% and 45% respectively when compared with P1.
3. Also, significant improvement in the secant stiffness ( $K_u$ ) is noticed with increase of thickness of FRP sheet. The predicted increase in the secant stiffness ( $K_u$ ) is 20% and 27% for specimens P2 and P3 respectively compared to specimen P1.
4. Finally, as shown in Figure (2), the strain of the tension reinforcement ( $\epsilon_s$ ) is decreased by about 19% and 21% for specimens P2 and P3 respectively, compared to the control specimen P1 at the same load.

### 3.2 Angle of FRP Sheets

Three deep beams strengthened with CFRP sheets with different fiber orientations are analyzed. The first deep beam (P1) has no FRP sheets, the second-deep beam (P2) strengthened with fibers aligned at 90 degrees to the longitudinal axis of beam and the third deep beam (P4) strengthened with fibers applied perpendicular to the predicted shear crack; at 45 degrees to the longitudinal axis of beam. The numerical load-deflection curves and load-steel strain curves for the analyzed specimens are shown in Figure (3). The following points are noticed based on the comparison between strengthened specimens P2 and P4 with the reference control specimen P1:

1. The strengthening with fibers perpendicular to shear cracks improves the shear capacity of the deep beams at all levels. An increment in the load capacity by 79% and 148% has been observed for specimen P2 and P4 respectively when compared with control specimen P1 at the cracking level, and by 69% and 95% at the ultimate level.
2. The strengthening with fibers perpendicular to shear cracks increases the deflection at all levels. At cracking level, the deflection ( $\Delta_{cr}$ ) is increased for specimens P2 and P4 by 39% and 40% respectively. Also, at the ultimate level, the deflection ( $\Delta_u$ ) is increased for specimens P2 and P4 by 40% and 47% respectively when compared with specimen P1.
3. Also, an enhancement in the secant stiffness ( $K_u$ ) is noticed. The expected increase in the secant stiffness ( $K_u$ ) is 20% and 33% for specimens P2 and P4 respectively compared to specimen P1.

4. As shown in Figure (3), the strain of the longitudinal reinforcement ( $\epsilon_s$ ) is decreased by about 19% and 21% for specimen P2 and P4 respectively compared to the control specimen P1 at the same load.

### 3.3 Length of FRP Sheets

Four deep beams strengthened with CFRP sheets which applied within quarter, half and full length of shear span are analyzed. The first deep beam (P1) has no FRP sheets, the second beam (P2) has CFRP sheet within full shear span, the third beam (P5) has sheet within half shear span and the last deep beam (P6) has sheet occupied only quarter shear span. Figure (4) presents the predicted load-deflection curves and load-steel strain curves for deep beams P1, P2, P5 and P6. The predicted failure mode is shear failure. The failure mode is characterized by inclined crack connecting between the load and the support for control specimen and specimens strengthened within quarter and half shear span. The partial delamination and the rapid rupture of CFRP sheets were identified for the specimen strengthened within full shear span. The following points are concluded from comparison of strengthened specimens (P2, P5 and P6) with control specimen P1:

1. An enhancement in the cracking shear capacity by 79%, 39% and 16% has been observed for specimens P2, P5 and P6 respectively when compared with specimen P1, and in the ultimate shear capacity by 69%, 40% and 21% for deep beams P2, P5 and P6 respectively.
2. At cracking level, the deflection ( $\Delta_{cr}$ ) is increased for specimens P2, P5 and P6 by 39%, 26% and 13% respectively. Also, at the ultimate level, the deflection ( $\Delta_u$ ) is increased for specimens P2, P5 and P6 by 40%, 24% and 9% respectively when compared with specimen P1.
3. Also, significant improvement in the secant stiffness ( $K_u$ ) is noticed. The increase in the secant stiffness ( $K_u$ ) is 20%, 13% and 12% for specimens P2, P5 and P6 respectively compared to specimen P1.
4. As shown in Figure (4), the strain of the tension reinforcement ( $\epsilon_s$ ) is decreased by about 19%, 17% and 15% for specimen P2, P5 and P6 respectively compared to the control specimen P1 at the same load level.

### 3.4 FRP Sheets Material

Three deep beams strengthened with different types of FRP sheets are analyzed. The first deep beam (P1) has no FRP sheets, the second-deep beam (P2) strengthened with CFRP sheets and the third deep beam (P7) strengthened with GFRP sheets. The numerical load-deflection curves and load-steel strain curves for the analyzed specimens are shown in Figure (5). The following points are noticed based on the comparison between strengthened specimens P2 and P7 with the control specimen P1:

1. An increment in the load capacity by 79% and 26% has been observed for specimen P2 and P7 respectively when compared with control specimen P1 at the cracking level, and by 69% and 37% at the ultimate level.

2. At cracking level, the deflection ( $\Delta_{cr}$ ) is increased for specimens P2 and P7 by 39% and 21% respectively. Also, at the ultimate level, the deflection ( $\Delta_u$ ) is increased for specimens P2 and P7 by 40% and 30% respectively when compared with specimen P1.
3. Also, an enhancement in the secant stiffness ( $K_u$ ) is noticed. The expected increase in the secant stiffness ( $K_u$ ) is 20% and 5% for specimens P2 and P7 respectively compared to specimen P1.
4. As shown in Figure (5), the strain of the longitudinal steel ( $\epsilon_s$ ) is decreased by about 19% and 8% for specimens P2 and P7 respectively compared to the control specimen P1 at the same load.

#### **4. Effect of FRP Strips Parameters**

In this section, the effects of FRP strips thickness, FRP strips angle, spacing between FRP strips and FRP strips material are investigated. The basic specimens used in this section, are the deep beam (P8) that has no FRP strips, and the deep beam (P9) which strengthened with CFRP strips. The experimental results for these beams are reported in [6]. Typical geometrical details and 3-D finite element models are shown in Figure (6) for deep beams (P8, P9, P10, P11, P12 and P13).

##### **4.1 Thickness of FRP Strips**

Three deep beams strengthened with different thickness of FRP strips are considered. The deep beam P8 is the un-strengthened control specimen. The FRP strip thickness is considered as 0.13mm and 0.26mm for P9 and P10 respectively. The predicted load-deflection curves and load-steel strain curves for the deep beams are shown in Figure (7). The following main points are obtained from the comparison between strengthened specimens P9 and P10 with the reference specimen P8:

1. Generally, the increase of FRP strips thickness improves the shear capacity at all levels. Compared to P8, an enhancement in the shear capacity is observed for specimens P9 and P10 respectively by 40% and 74% at cracking level, and by 32% and 51% at ultimate level.
2. Comparing the mid-span deflections of deep beams at the same load, the deflections are inversely proportional to the thickness of FRP strips as shown in Figure (7). It was found that the vertical deflection decreased for specimens P9 and P10 by about 33% and 56% respectively, compared to the control specimen P8.
3. Also, significant improvement in the secant stiffness ( $K_u$ ) is noticed with the increase of thickness of FRP strips. The predicted increase in the secant stiffness ( $K_u$ ) is 47% and 75% for specimens P9 and P10 respectively compared to P8.
4. As shown in Figure (7), the strain of tension reinforcement ( $\epsilon_s$ ) is decreased by about 35% and 45% for specimens P9 and P10 respectively, compared to the specimen P8 at the same load.

##### **4.2 Angle of FRP Strips**

Three deep beams strengthened with CFRP strips with different FRP strips angle are analyzed. The first deep beam (P8) has no FRP strips, the second-deep beam (P9)

strengthened with FRP strips aligned at 90 degrees to the longitudinal axis of beam and the third deep beam (P11) strengthened with CFRP strips applied perpendicular to the predicted shear crack; at 45 degrees to the longitudinal axis of beam. The predicted load-deflection curves and load-steel strain curves are shown in Figure (8). The following concluded points are obtained from the comparison between strengthened specimens P9 and P11 with the control specimen P8:

1. The strengthening with FRP strips perpendicular to shear cracks improves the shear capacity of the deep beams at all levels. An increase in the load capacity by 40% and 74% has been observed for specimens P9 and P11 respectively when compared with control specimen P8 at the cracking level and by 32% and 53% at the ultimate level.
2. The mid-span deflections of deep beams were inversely proportional to beam strengthening at the same load as shown in Figure (8). It was found that the vertical mid-span deflection decreased for specimens P9 and P11 by about 33% and 55% respectively, compared to control specimen P8.
3. An enhancement in the secant stiffness ( $K_u$ ) is noticed. The expected increase in the secant stiffness ( $K_u$ ) is 47% and 65% for specimens P9 and P11 respectively compared to the reference specimen P8.
4. As shown in Figure (8), the strain of longitudinal reinforcement ( $\epsilon_s$ ) is decreased by about 35% for both specimens P9 and P11 compared to the control specimen P8 at the same load.

### **4.3 Spacing between FRP Strips**

Three deep beams strengthened with CFRP strips which applied within different spacing are analyzed. The first deep beam (P8) has no FRP strips, the second-deep beam (P9) strengthened with CFRP strips within shear span every 100 mm, and the third deep beam (P12) retrofitted with CFRP strips within shear span every 25 mm. The predicted load-deflection curves and load-steel strain curves are shown in Figure (9). Based on the numerical results of strengthened deep beams P9 and P12 with respect to deep beam P8, the following concluded points are obtained:

1. Compared with P8, an improvement in the shear capacity for specimens P9 and P12 is observed by 40% and 89% respectively at cracking level, and by 32% and 66% respectively at the ultimate level.
2. Comparing the mid-span deflections of deep beams at the same load level, the deflections were inversely proportional to beam strengthening as shown in Figure (9). It was found that the vertical mid-span deflection decreased for specimens P9 and P12 by about 33% and 59% respectively, compared to the control specimen P8 at the same load.
3. Also, significant improvement in the secant stiffness ( $K_u$ ) is noticed. The expected increase in the secant stiffness ( $K_u$ ) is 47% and 77% for specimens P9 and P12 respectively, compared to P8.
4. As shown in Figure (9), the strain of the tension steel ( $\epsilon_s$ ) is decreased by about 35% and 40% respectively for specimens P9 and P12, compared to specimen P8 at the same load.

#### 4.4 FRP Strips Material

Three deep beams strengthened with different types of FRP strips are studied. The first deep beam (P8) has no FRP strips, the second-deep beam (P9) strengthened with CFRP strips and the third deep beam (P13) strengthened with GFRP strips. The predicted load-deflection curves and load-steel strain curves for the three deep beams are shown in Figure (10). The following main points are obtained from the comparison between strengthened specimens (P9 and P13) with the reference specimen P8:

1. Compared with P8, an increase in the shear capacity is observed for specimens P9 and P13 respectively by 40% and 17% at the cracking level, and by 32% and 17% at the ultimate level.
2. The mid-span deflections of deep beams were inversely proportional to beam strengthening at the same load level as shown in Figure (10). It was found that the vertical mid-span deflection decreased for specimens P9 and P13 by about 33% and 13% respectively, compared to the control specimen P8.
3. An enhancement in the secant stiffness ( $K_u$ ) is noticed. The expected increase in the secant stiffness ( $K_u$ ) is 47% and 23% for specimens P9 and P13 respectively compared to the reference specimen P8.
4. As shown in Figure (10), the strain of the longitudinal steel ( $\epsilon_s$ ) is decreased by about 35% and 34% for specimens P9 and P13 respectively compared to the control specimen P8 at the same load.

#### 5. Conclusions

From the extensive parametric shear studies on FRP-strengthened RC deep beams using ANSYS software, the following points are drawn:

1. Increasing FRP thickness in strengthened deep beams, enhances the ultimate shear capacity ( $P_u$ ) and the secant stiffness ( $K_u$ ). Compared to un-strengthened deep beam, the use of sheets with thickness of 0.17mm and 0.34mm, improves the shear capacity by 69% and 85% respectively, and enhances the secant stiffness by 20% and 27% respectively. Compared to un-strengthened deep beam, the FRP strips with thickness of 0.13mm and 0.26mm increase the shear capacity by 32% and 51% respectively, and enhance the secant stiffness by 47% and 75% respectively.
2. An enhancement in the shear capacity and secant stiffness is noticed by strengthening by FRP applied perpendicular to the predicted shear crack. Strengthening using FRP sheets with fibers applied at an angle 90 degree and 45 degrees to the longitudinal axis of the beam, increases the ultimate load capacity by 69% and 95%, respectively, and enhances the secant stiffness by 20% and 33% respectively, compared to un-strengthened beam. Compared to un-strengthened specimen, strengthening using strips applied at an angle 90 degree and 45 degrees to the longitudinal axis of beam improves the ultimate load capacity by 32% and 53%, respectively and increases the secant stiffness by 47% and 65% respectively.
3. The efficiency of shear strengthening with FRP sheets or strips, increases as the strengthening length increases. Compared with un-strengthened specimen, strengthening using FRP sheets within full, half and quarter shear span, improves the

ultimate load capacity by 69%, 40% and 21% respectively, and enhances the secant stiffness by 20%, 13% and 12% respectively. Strengthening using FRP strips applied within shear span every 100mm and 25mm, increases the ultimate shear capacity by 32% and 66% respectively, and enhanced the secant stiffness by 47% and 77% respectively, compared with un-strengthened specimen.

4. Higher ultimate loads are achieved for deep beams strengthened with CFRP sheets or strips compared with specimen strengthened with GFRP. Compared to un-strengthened specimen, CFRP and GFRP sheets improves the ultimate load capacity by 69% and 37% respectively, and upgrades the secant stiffness by 20% and 5% respectively. The use of CFRP and GFRP strips enhances the ultimate load capacity by 32% and 17% respectively, and improves the secant stiffness by 47% and 23% respectively, compared to the un-strengthened specimen.

## 6. References

1. Javed, M. A., Irfan, M., Khalid, S., Chen, Y., and Ahmed, S., "An Experimental Study on the Shear Strengthening of Reinforced Concrete Deep Beams with Carbon Fiber Reinforced Polymers", *Journal of Korean Society of Civil Engineers* (2016), 20(7):2802-2810.
2. Al-Ahmed, A. H. A., and Al-Jburi, M.H.M., "Behavior of Reinforced Concrete Deep Beams Strengthened with Carbon Fiber Reinforced Polymer Strips", *Journal of Engineering*, Vol. 22, No.8, August 2016, pp.37-53.
3. Elsonbaty, M. M., Montaser, W. M., and Zaher, A. H., "Strengthening of RC Deep Beams Using CFRP and GFRP", *Al-Azhar University Civil Engineering Research Magazine (CERM)*, Vol. 40, No.4, October 2018.
4. Islam, M.R., Mansur, M.A., and Maalej, M., "Shear Strengthening of RC Deep Beams Using Externally Bonded FRP Systems", *Journal of Cement and Concrete Composites* 27 (2005) 413-420.
5. Al-Ghanim, H., Abdel-Jaber, M., and Alqam, M., "Shear Strengthening of Reinforced Concrete Deep Beams Using Carbon Fiber Reinforced Polymers", *Journal of Modern Applied Science*, Vol. 11, No.10, 2017.
6. Rasheed, M. M., "Retrofit of Reinforced Concrete Deep Beams with Different Shear Reinforcement by Using CFRP", *Journal of Civil and Environment Research*, Vol. 8, No.5, 2016, pp.6-14.
7. ANSYS–Release Version 12.1.0, "A Finite Element Computer Software and User Manual for Nonlinear Structural Analysis", ANSYS Inc. Canonsburg, PA., (2009).
8. Fathi, M.G., "Shear Assessment of FRP-Strengthened Reinforced Concrete Deep Beams", M.Sc. Thesis to be Submitted, Benha University, Faculty of Engineering, Shoubra, Egypt, 2021.
9. Desayi, P., and Krishnan, S., "Equation for the Stress-Strain Curve of Concrete", *Journal of the American Concrete Institute*, Vol. 61, No.3, pp. 345-350, March, 1964.
10. Evans, R. H., and Marathe, M. S., "Micro-Cracking and Stress-Strain Curves for Concrete in Tension", *Journal of Materials and Structures, Research and Testing (RILEM, Paris)*, Vol.1, No.1, Jan.-Feb. 1986, pp.61-64.



**Table 1: Structural Element Types Used in the Numerical Models**

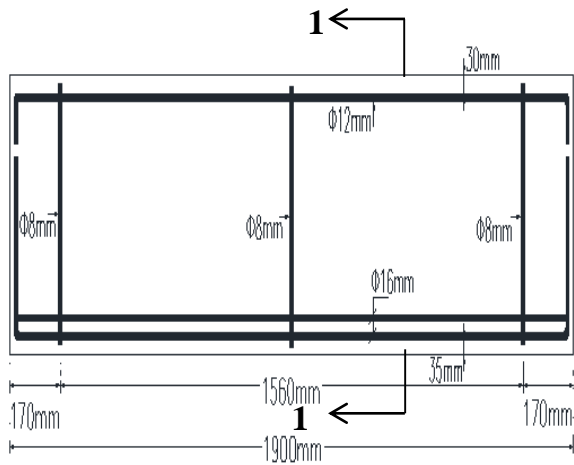
<b>Material</b>	<b>Structural Element</b>
<b>Concrete</b>	SOLID 65
<b>Steel bars</b>	LINK 8
<b>Bearing and Loading Plates</b>	SOLID 45
<b>FRP Layers</b>	SHELL 41

**Table (2): Input Data for Deep Beams Strengthened by FRP Sheets**

<b>Deep Beam</b>	$f_c'$ (MPa)	$f_y$ (MPa)	$\frac{a}{d}$	$\rho_s$ %	<i>FRP Sheet Thickness</i> (mm)	<i>Fiber Angle</i>	<i>FRP Strengthening Length</i>	<i>FRP Material</i>
P1	30	400	1.19	1.89	---	---	---	---
P2	30	400	1.19	1.89	0.17	90°	100%	CFRP
P3	30	400	1.19	1.89	0.34	90°	100%	CFRP
P4	30	400	1.19	1.89	0.17	45°	100%	CFRP
P5	30	400	1.19	1.89	0.17	90°	50%	CFRP
P6	30	400	1.19	1.89	0.17	90°	25%	CFRP
P7	30	400	1.19	1.89	0.17	90°	100%	GFRP

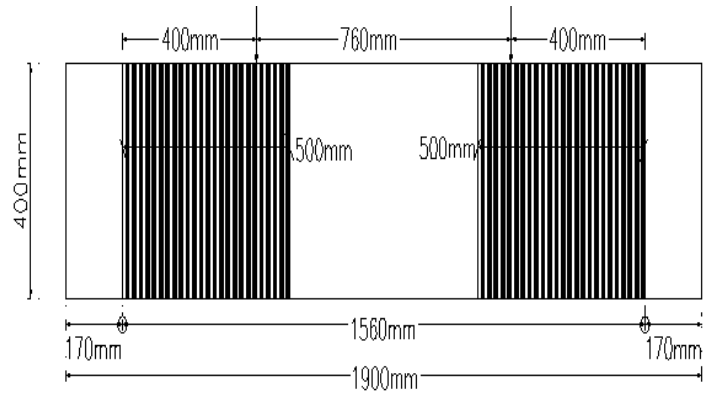
**Table (3): Input Data for Deep Beams Strengthened by FRP Strips**

<b>Deep Beam</b>	<i>FRP Strip Thickness</i> (mm)	<i>FRP Strips Angle(<math>\theta</math>)</i> <i>with X-axis</i>	<i>FRP Strips spacing</i> (mm)	<i>FRP Material</i>
<b>P8</b>	----	----	----	----
<b>P9</b>	0.13	90	100	CFRP
<b>P10</b>	0.26	90	100	CFRP
<b>P11</b>	0.13	45	100	CFRP
<b>P12</b>	0.13	90	25	CFRP
<b>P13</b>	0.13	90	100	GFRP

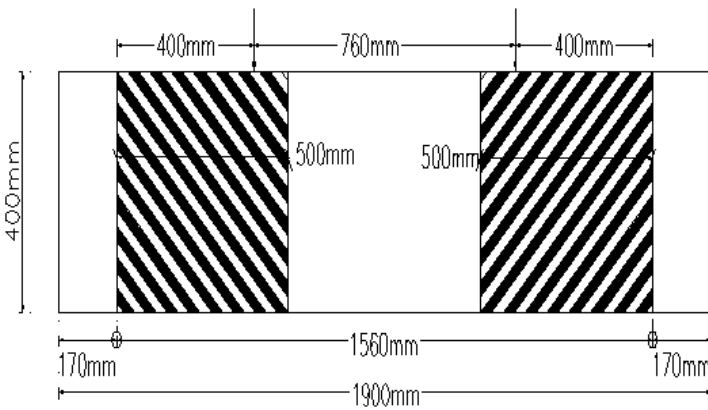


(a) Deep Beam (P1)

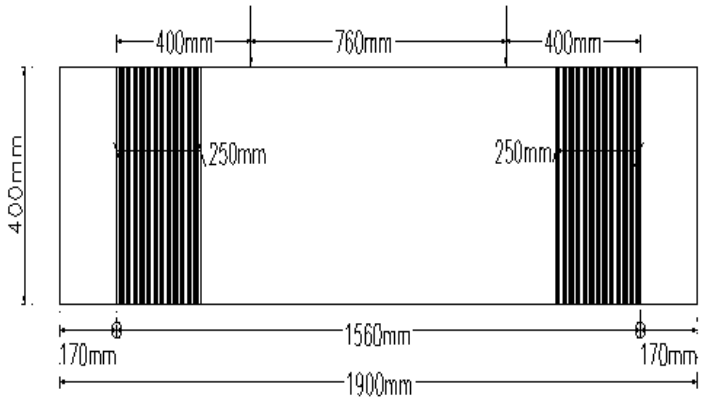
Sec. 1-1



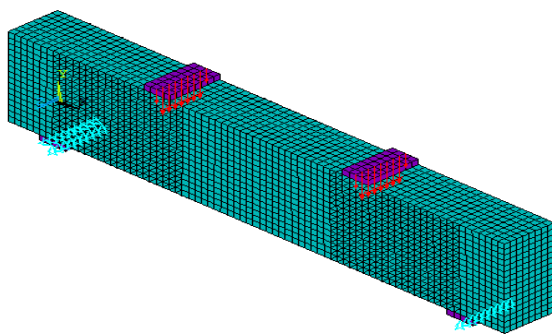
(b) Deep Beams (P2, P3 and P7)



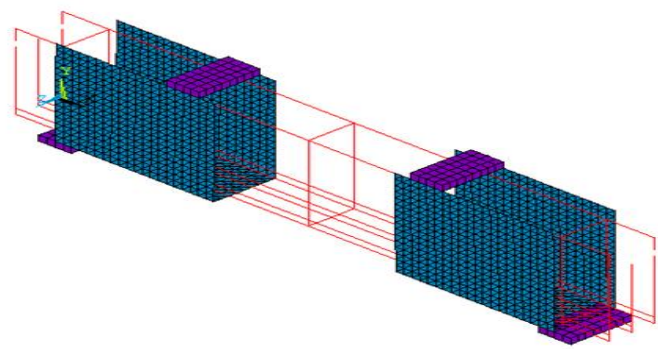
(c) Deep Beam (P4)



(d) Deep Beam (P5)



(e) FE Idealization for Concrete, Loading and Bearing Plates



(f) FE Idealization for FRP Sheets, Top and Bottom Reinforcement and Stirrups

**Figure (1) Typical Geometrical Details and F.E. Models for Deep Beams P1, P2, P3, P4, P5 and P7**

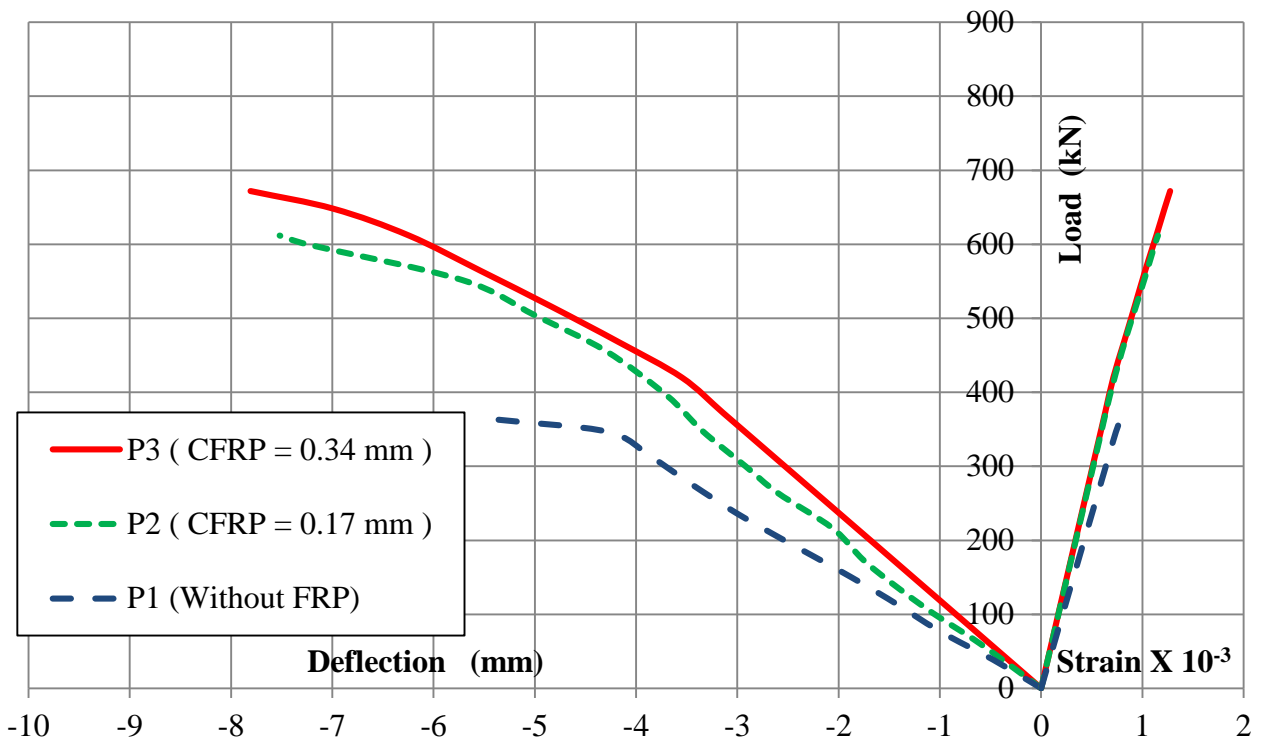


**Figure (2) Effect of FRP Sheets Thickness on the Load-Deflection and the Load-Steel Strain Curves for Deep Beams P1, P2 and P3**

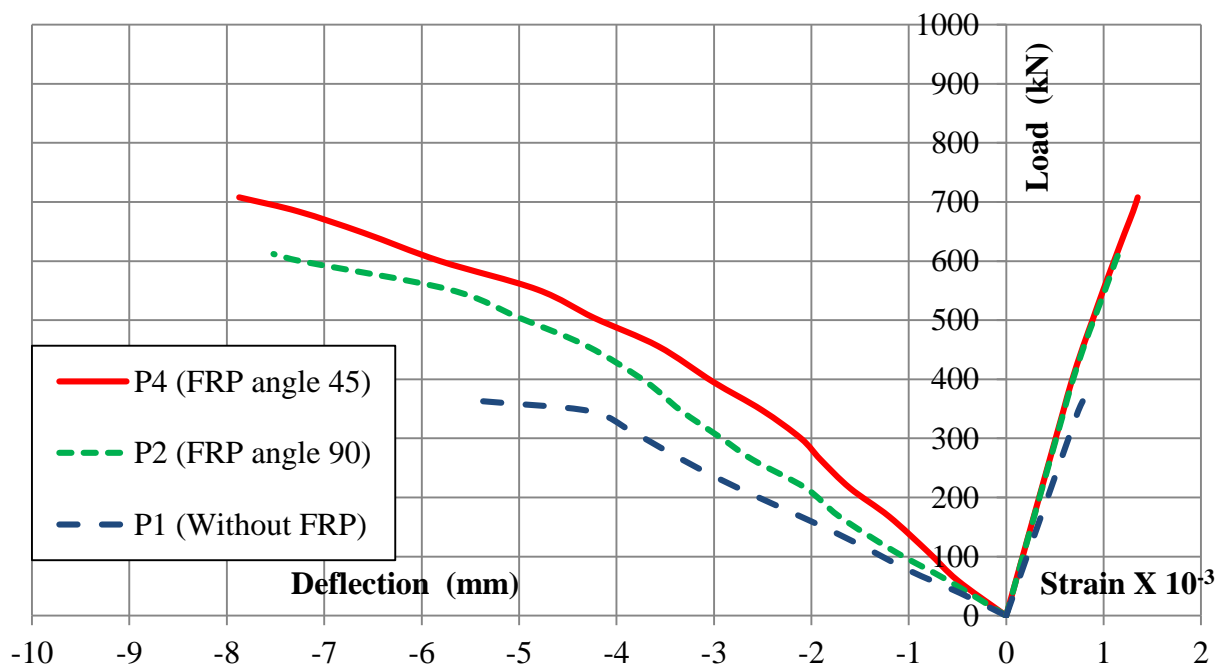


**Figure (3) Effect of Fiber Angle on the Load-Deflection and the Load-Steel Strain Curves for Deep Beams P1, P2 and P4**

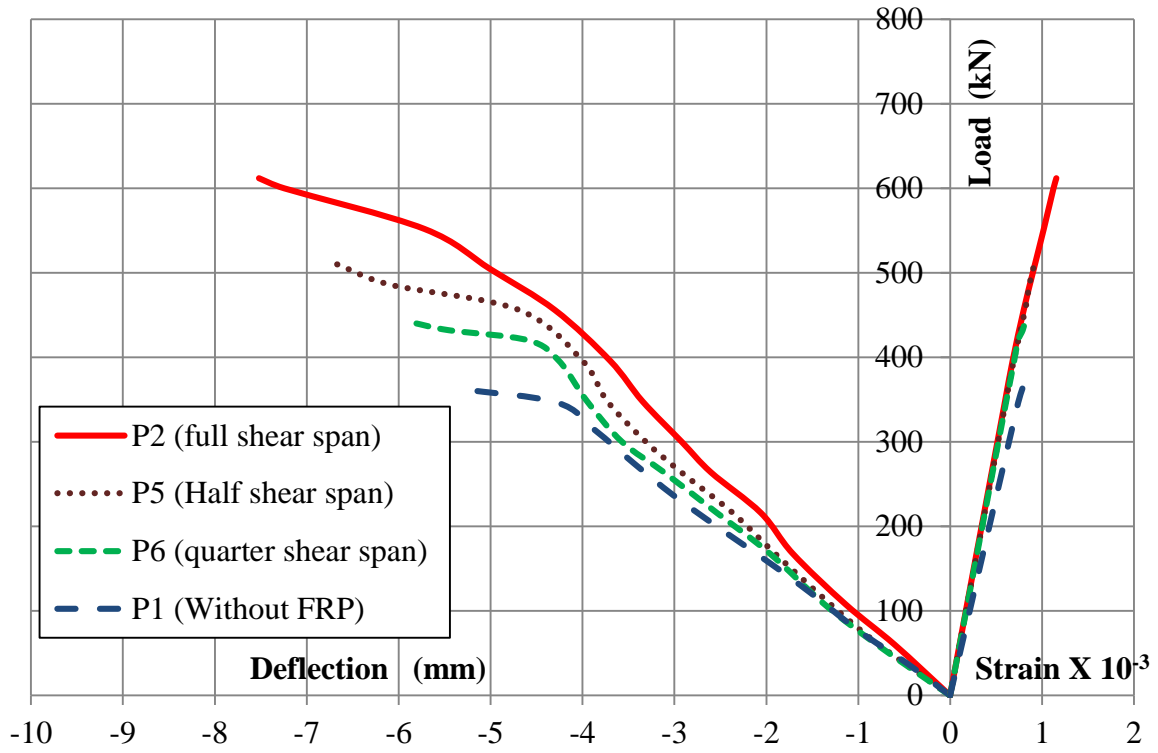


**Figure (4) Effect of FRP Strengthening Length on the Load-Deflection and the Load-Steel Strain Curves for Deep Beams P1, P2, P5 and P6**

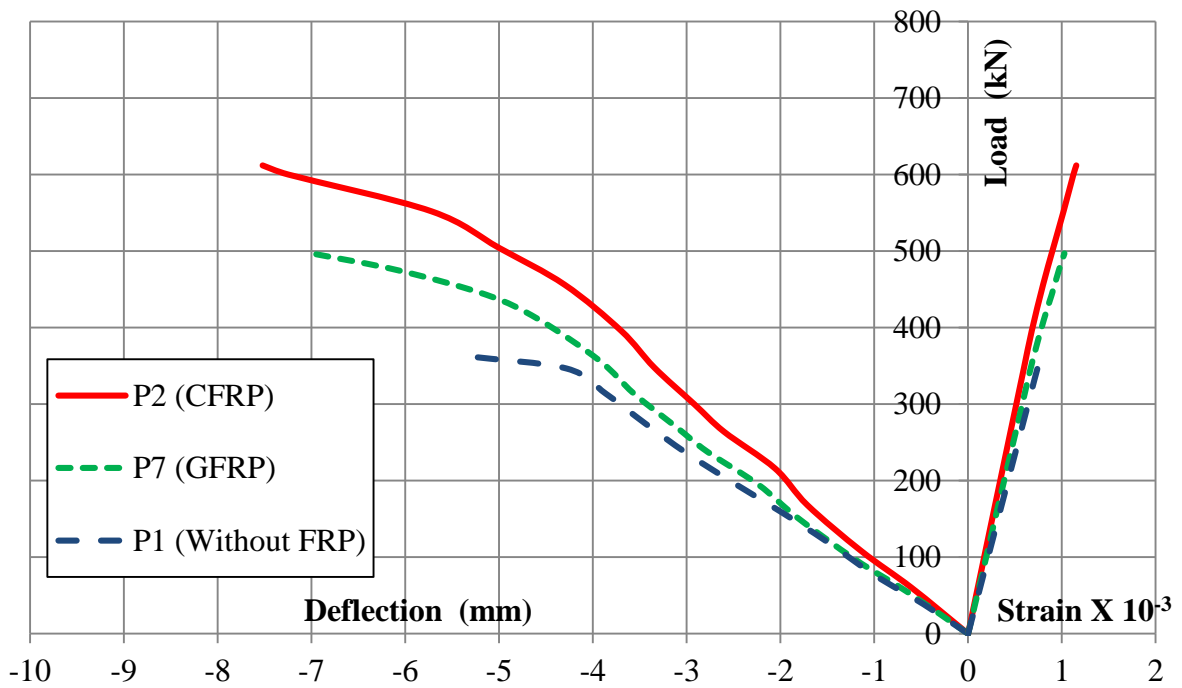
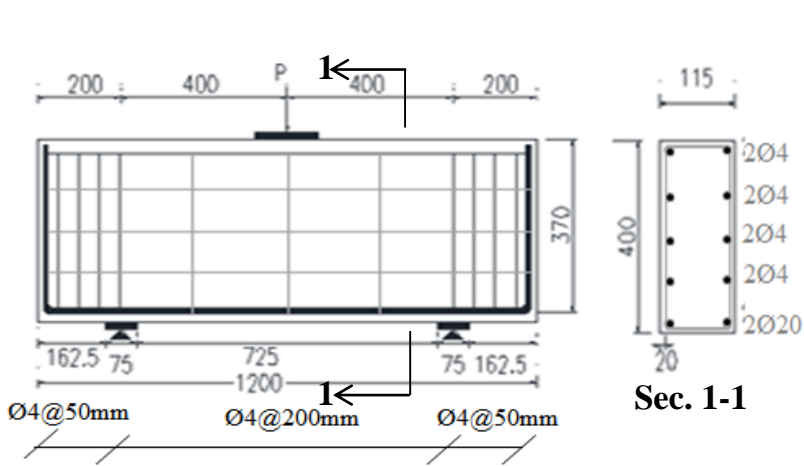
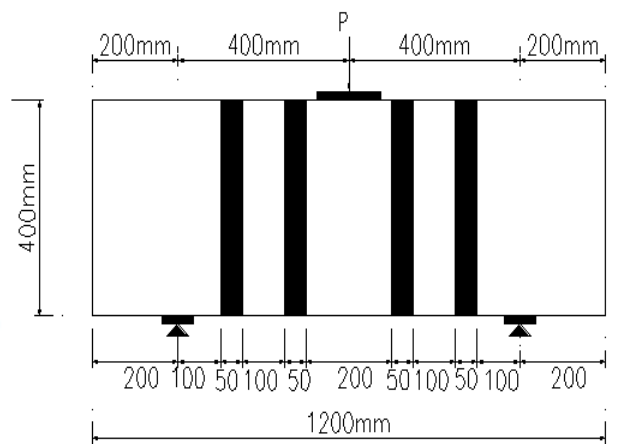


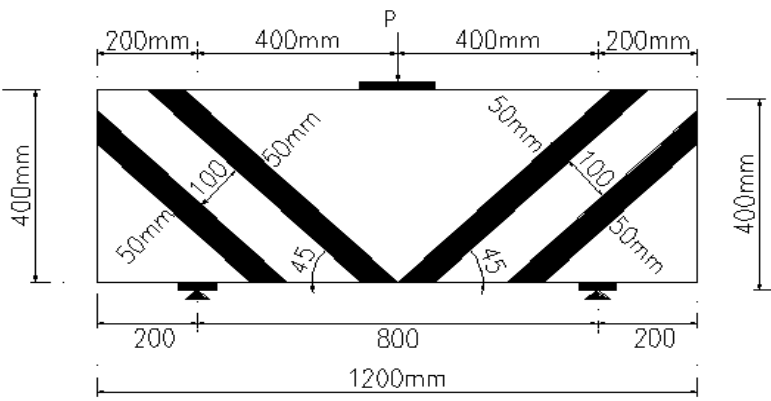
**Figure (5) Effect of FRP Sheets Material on the Load-Deflection and the Load-Steel Strain Curves for Deep Beams P1, P2 and P7**



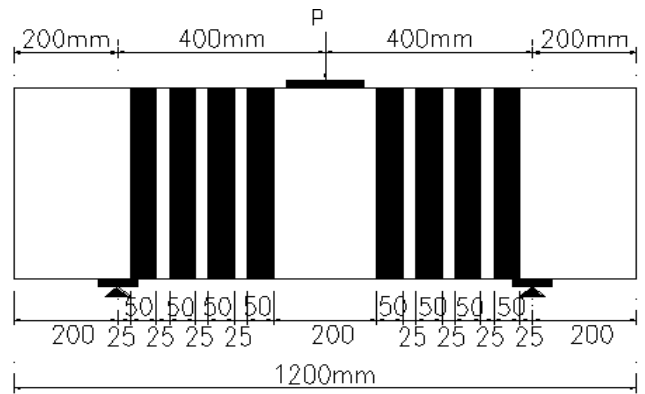
**(a) Deep Beam (P8)**



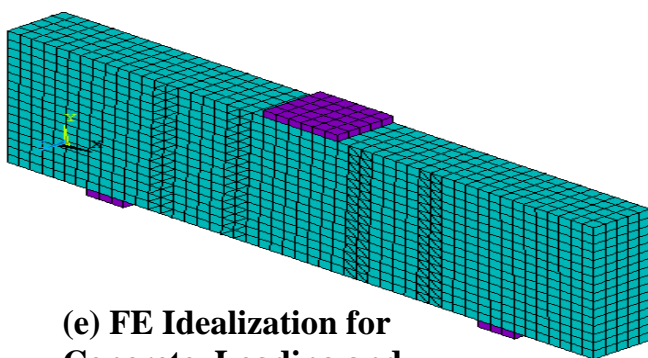
**(b) Deep Beams (P9, P10 and P13)**



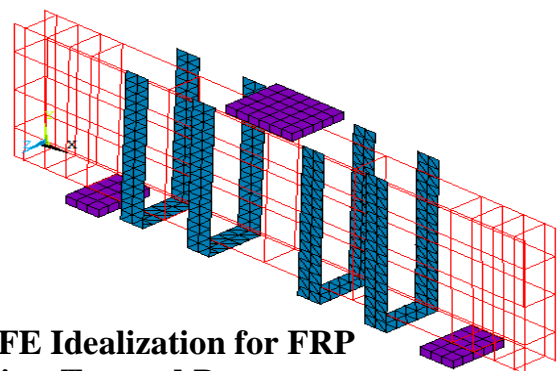
**(c) Deep Beam (P11)**



**(d) Deep Beam (P12)**



**(e) FE Idealization for Concrete, Loading and Bearing Plates**



**(f) FE Idealization for FRP Strips, Top and Bottom Reinforcement and Stirrups**

**Figure (6) Typical Geometrical Details and F.E. Models for Deep Beams P8, P9, P10, P11, P12 and P13**

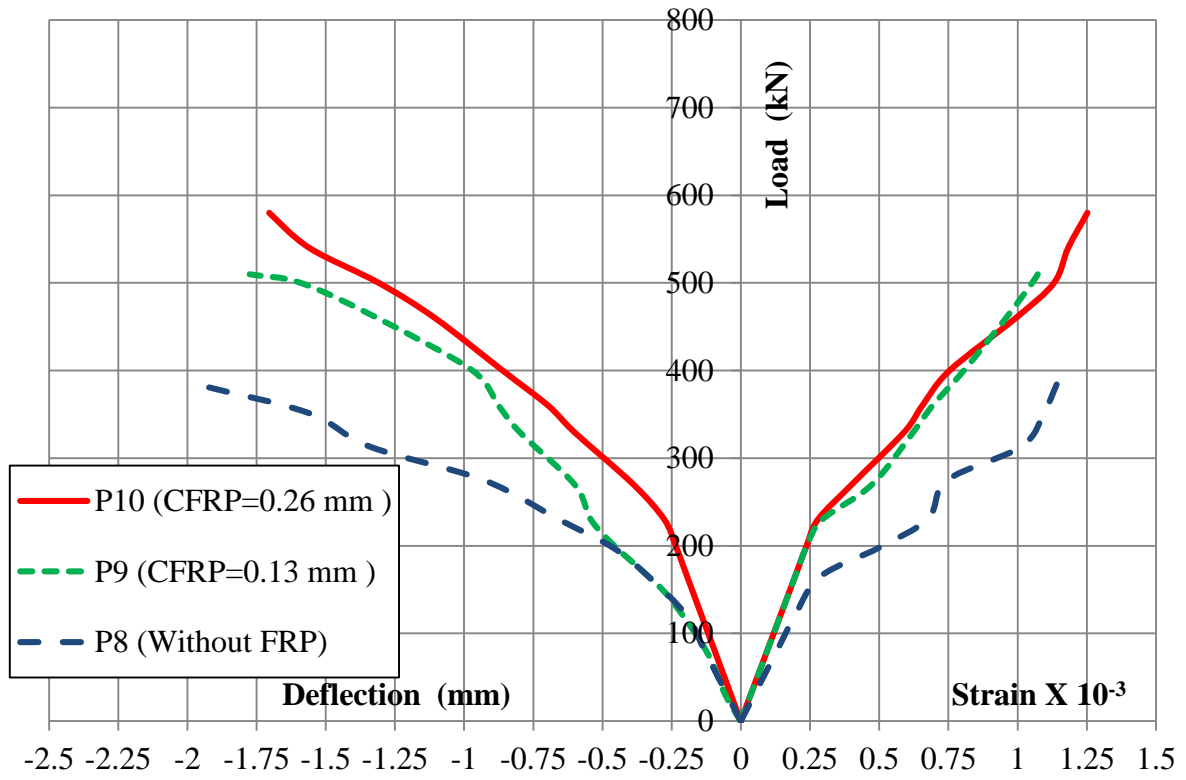


**Figure (7) Effect of FRP Strips Thickness on the Load-Deflection and the Load-Steel Strain Curves for Deep Beams P8, P9 and P10**

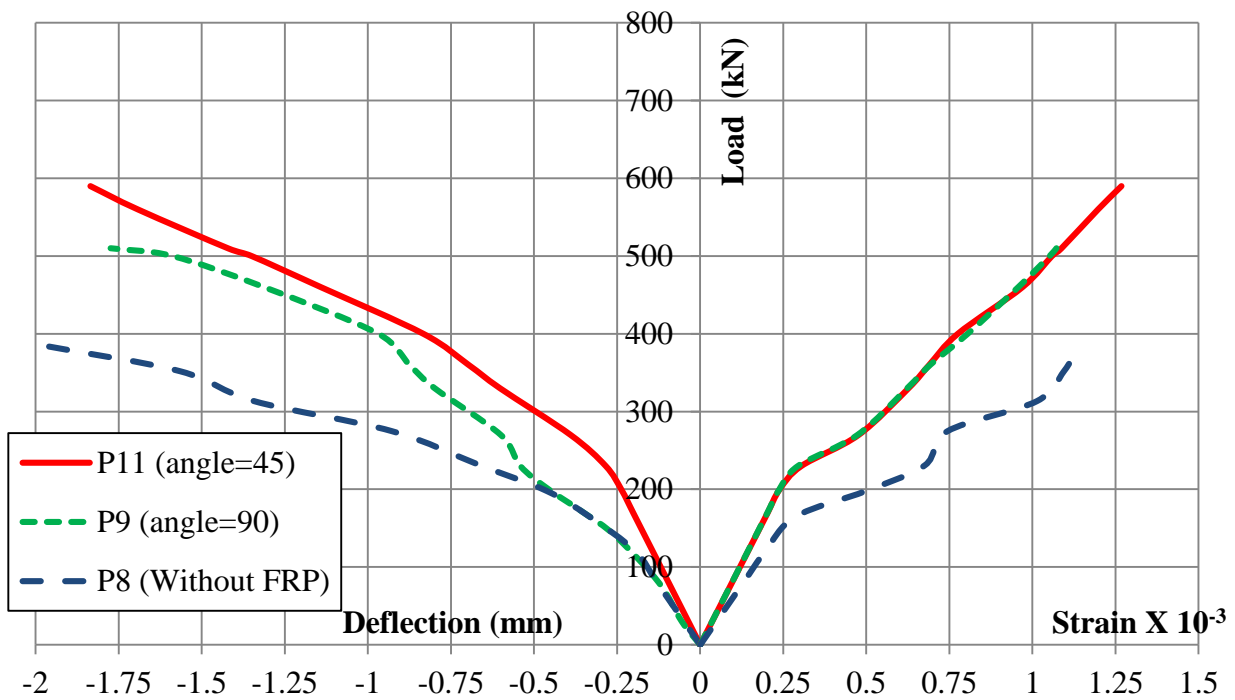


**Figure (8) Effect of FRP Strips Angle on the Load-Deflection and the Load-Steel Strain Curves for Deep Beams P8, P9 and P11**

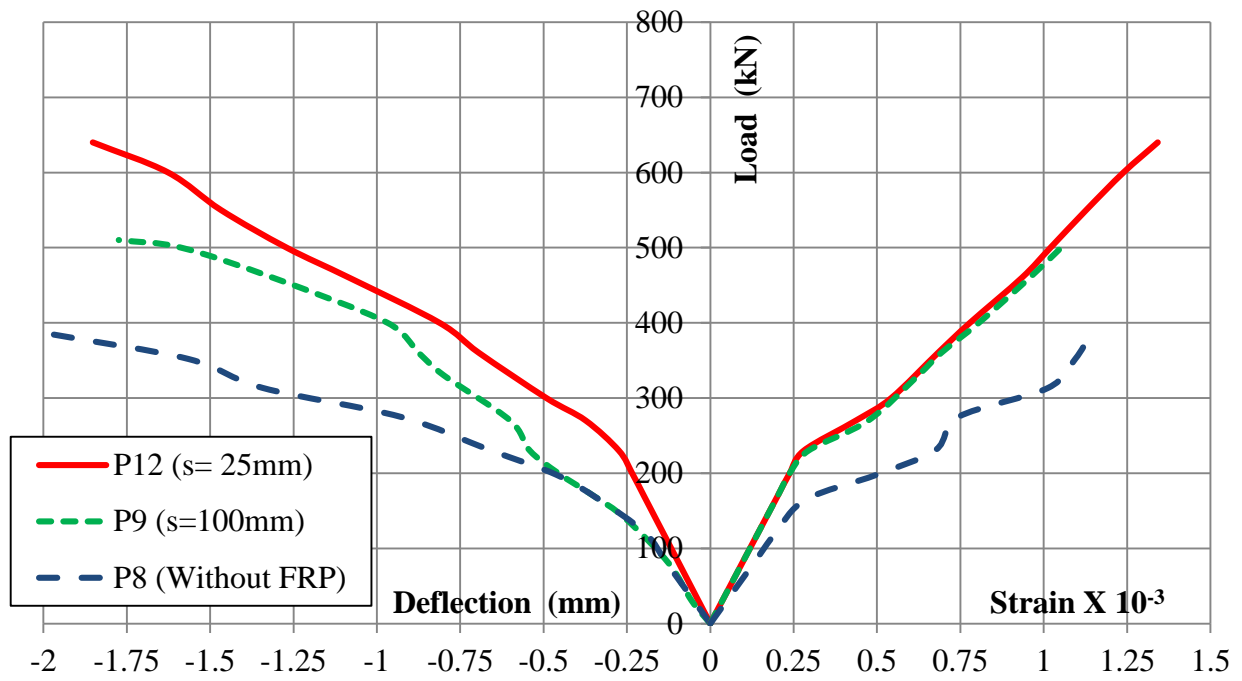


**Figure (9) Effect of FRP Strips Spacing (S) on the Load-Deflection and the Load-Steel Strain Curves for Deep Beams P8, P9 and P12**

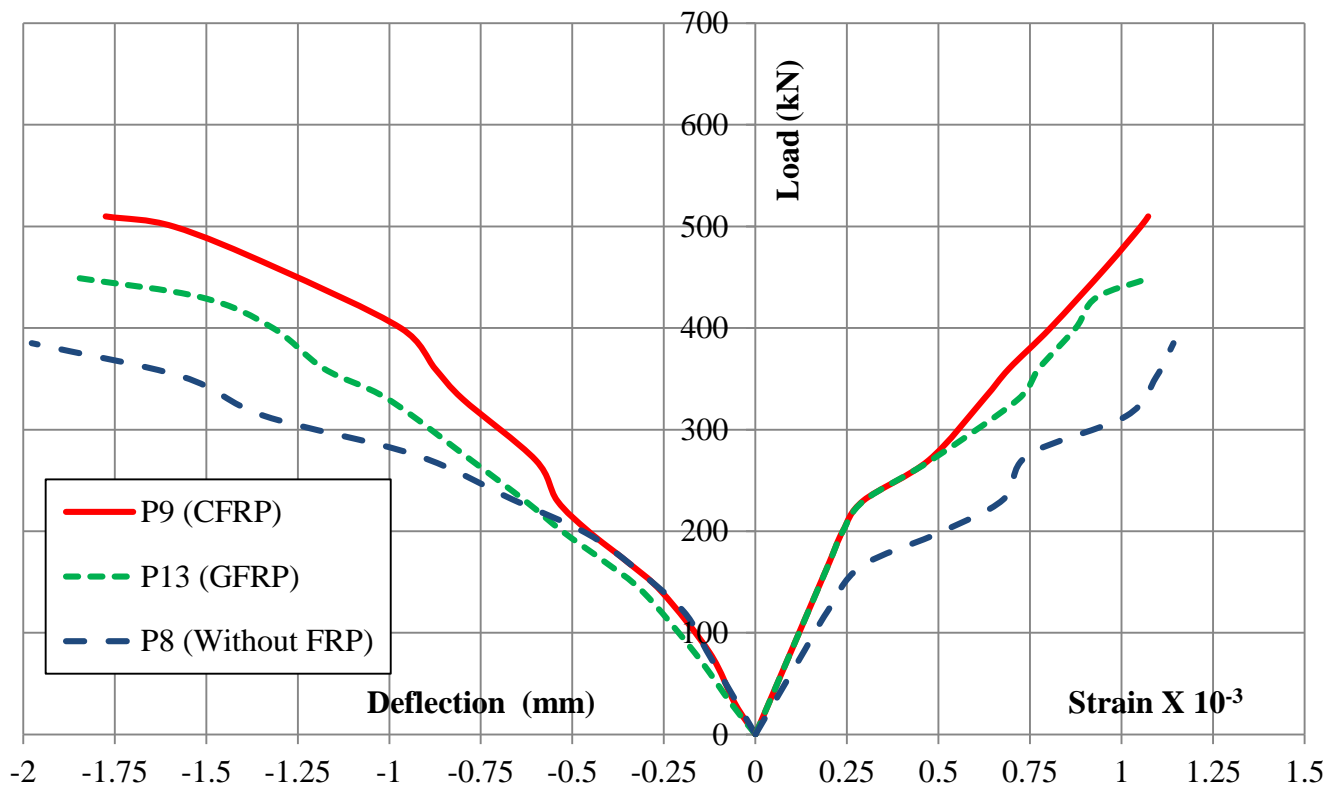


**Figure (10) Effect of FRP Strips Material on the Load-Deflection and the Load-Steel Strain Curves for Deep Beams P8, P9 and P13**